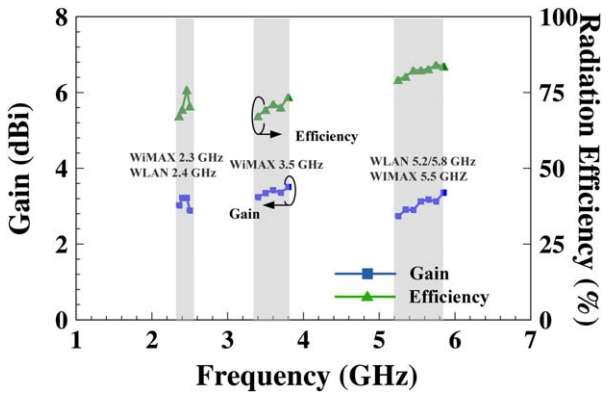

Figure 11 Measured peak gains and efficiencies of proposed antenna across all bands of interest. [Color figure can be viewed in the online issue, which is available at wileyonlinelibrary.com]

WLAN 2.4 GHz operating band has exhibited a small gain and efficiency variation of 2.7–3.2 dBi and 70%–75%, respectively. Slight increment in gain and efficiency of 3.1–3.5 dBi and 65%–73% were also observed, respectively, across the WiMAX 3.5 GHz operating band. Similar trend were observed for the WLAN 5.2/5.8 GHz and WiMAX 5.5 GHz operating bands, showing a stable increment in gain and efficiency of 2.8–3.3 dBi and 77%–84%, respectively.

5. CONCLUSION

A small size CPW-fed monopole antenna for WLAN 2.4/5.2/58 GHz and WiMAX 2.3/3.5/5.5 GHz operations has been successfully studied and implement. To achieve tripleband operation, four resonant modes were excited by implementing a modified U-shaped monopole structure with a parasitic element. Desirable impedance bandwidth was also further achieved by introducing two notches into the CPW ground planes. Besides the ability to yield broad 10-dB impedance bandwidth of approximately (17%–28%) for all three operating bands, peak gain and radiation efficiency of more than 2.7 dBi and 65%, respectively, were also measured across all bands of interest.

REFERENCES

1. J.H. Yoon, Y.C. Rhee, and Y.K. Jang, Compact monopole antenna design for WLAN/WiMAX triple-band operations, Microwave Opt Technol Lett 54 (2012), 1838–1846.
2. C.H. Ku, L.K. Li, and W.L. Mao, Compact monopole antenna with branch strips for WLAN/WiMAX operation, Microwave Opt Technol Lett 52 (2010), 1858–1861.
3. H.W. Liu, C.H. Ku, and C.F. Yang, Novel CPW-fed planar monopole antenna for WiMAX/WLAN applications, IEEE Antennas Wireless Propag Lett 9 (2010), 240–243.
4. W.S. Chen and K.Y. Ku, Band-rejected design of open slot antenna for WLAN/WiMAX applications, IEEE Trans Antennas Propag 56 (2008), 1163–1169.
5. P. Liu, Y. Zou, B. Xie, X. Liu, and B. Sun, Compact CPW-fed tri-band printed antenna with meandering split-ring slot for WiMAX/WLAN applications, IEEE Antennas Wireless Propag Lett 11 (2012), 1241–1244.
6. Y. Xu, Y.C. Jiao, and Y.C. Luan, Compact CPW-fed printed monopole antenna with triple-band characteristics for WLAN/WiMAX applications, Electron Lett 48 (2012), 1519–1520.

EIT IN HOLLOW-CORE FIBERS FOR OPTICAL COMMUNICATIONS DEVICES

Bruno D. Tiburcio,[1] Gil M. Fernandes,[1,2] Jorge Monteiro,[3] Silvia Rodrigues,[3] Mario Ferreira,[3] Margarida Facão,[3] M. Inês Carvalho,[4] and Armando N. Pinto[1,2]
[1] Instituto de Telecomunicações, Campus Universitário de Santiago, 3810-193 Aveiro, Portugal; Corresponding author: btib78@av.it.pt
[2] Department of Electronics, Telecommunications and Informatics, University of Aveiro, Campus Universitário de Santiago, 3810-193 Aveiro, Portugal
[3] Department of Physics, I3N, University of Aveiro, Campus Universitário de Santiago, 3810-193 Aveiro, Portugal
[4] DEEC/FEUP and INESC TEC Porto, University of Porto, Rua Dr. Roberto Frias, 4200-465 Porto, Portugal

Received 4 July 2014

ABSTRACT: *We developed an experimental setup for electromagnetically induced transparency able to manufacture microcells, suitable for optical fiber communications technology. A hollow-core photonic crystal fiber (HC-PCF) is filled with acetylene, to work in the 1500 nm telecommunications window. We used a HC-PCF with the mode-field diameter compatible with standard single-mode fibers, with the purpose of achieving low-loss splicing and enabling us to work at low pumping powers. This allows to induce a narrow transparency window, which can be spectrally adjusted and dynamically controlled.* © 2015 Wiley Periodicals, Inc. Microwave Opt Technol Lett 57:348–352, 2015; View this article online at wileyonlinelibrary.com. DOI 10.1002/mop.28836

Key words: *electromagnetically induced transparency; hollow-core photonic crystal fiber; low-loss splice; optical fiber communications*

1. INTRODUCTION

Electromagnetically induced transparency (EIT) is an optical effect, which provides a narrow spectral transparent window within an absorption medium [1]. In addition, a very sharp variation in dispersion is also created in this transparency window [2]. EIT has attracted considerable interest in recent years, offering a variety of potential practical applications, such as all-optical switching [3], wavelength converters [4], and light storage [5]. Despite the advances on EIT based in hollow-core photonic crystal fiber (HC-PCF), the development of experimental setups at telecommunications window, for optical processing, using fibers with mode-field diameter (MFD) compatible with the standard single-mode fibers (SMF), allowing to produce photonic microcells with lower losses, is still not deeply explored.

The first demonstration of EIT was presented using a high power pulsed laser interacting with Strontium vapor [1], and since then, EIT has been studied in various media, such as gas vapor cells [6] and Bose–Einstein condensates [7]. The light propagation can be changed from slow light to fast light regime using EIT [8], a periodic modulation of atomic absorption can be produced with these phenomena, inducing a Bragg reflection of the signal [9]. Furthermore, the time required to open the transmission window, that is, the rise time, was also estimated in several milliseconds in Rubidium gas [10].

New possibilities have arisen with the development of HC-PCF, as these fibers can be readily integrated with telecommunications fiber technology [11]. HC-PCFs have the ability to combine light confinement and long interaction length [11], changing the approach to experiments involving interactions between light and gas [2]. Several nonlinear processes suitable

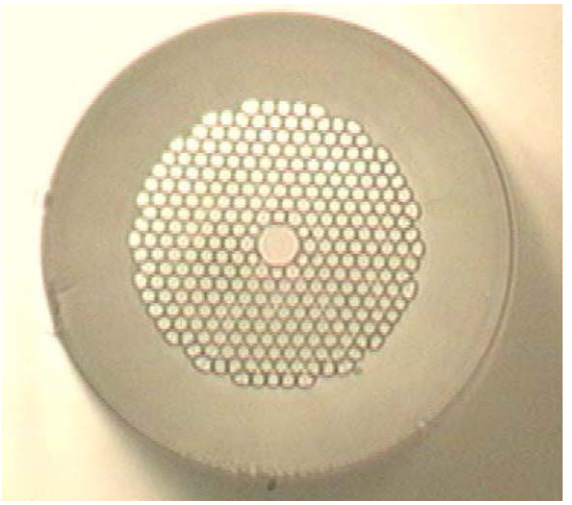

Figure 1 Optical microscope image of the HC-PCF cross section, used in our experiment. The geometrical parameters of the HC-PCF: core diameter of 10 μm, holey region with a diameter of 75 μm and cladding pitch of 4 μm. [Color figure can be viewed in the online issue, which is available at wileyonlinelibrary.com]

for optical signal processing were reported, including efficient Raman scattering at low power regimes, in HC-PCF filled with hydrogen [12], enhanced four-wave mixing of light pulses [13], compression of high energy pulses by self-phase modulation in noble gases [14], and efficient all-optical switching using slow light in HC-PCF filled with Rubidium [15]. To exploit EIT in optical communications, the acetylene (C_2H_2) has been investigated in HC-PCF, due to its spectral overlap with the low-loss fiber telecommunications window [16]. Acetylene is a symmetric molecule and has clean rovibrational transitions in this range [17], and besides that, can stay for a long time inside the fiber without significant leaks [18]. In acetylene-filled HC-PCF, it was reported that the pulse delays at telecommunications wavelengths, in which a delay of 800 ps was achieved with both end faces of the fiber opened to gas inlet, using a HC-PCF with a core diameter of 12 μm [11]. It was also reported the observation of EIT with 70% of transparency, with one end face opened and the other one spliced to a SMF, in a HC-PCF with 20 μm of core diameter [2], and a 20 m acetylene-filled photonic microcell, with 13 μm of core diameter and both end faces spliced, that was used to obtain delayed and advanced light pulses [19].

We implemented an experimental setup, which enables the gas injection into the core of the HC-PCF, to observe EIT. The HC-PCF was chosen to have the MFD most compatible with the SMF, allowing us to perform a low-loss splice, and consequently, able to work at low pumping powers. We induced a transparency in a 1500 nm telecommunications window. It was achieved a narrow transparent spectral peak, that can be spectrally adjusted and dynamically controlled. This configuration opens the possibility to manufacture photonic microcells, to implement EIT in optical communications, due to its portability and potentiality to develop all-fiber devices for all-optical signal processing.

This article is organized in four sections. In Section 2, we present the experimental setup and the procedure used to characterize EIT. In Section 3, we show the experimental results and its discussion. The conclusions are presented in Section 4.

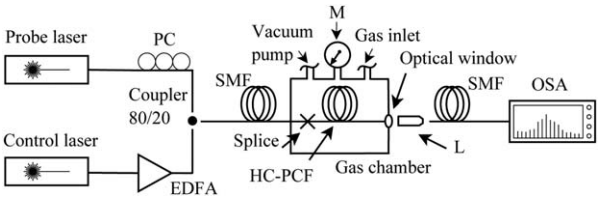

Figure 2 Schematic diagram of the experimental setup. Two CW lasers, probe and control fields, are coupled to launch the light via the SMF spliced to the HC-PCF. The output is aligned through an optical window with other SMF to be detected. PC: polarization controller; L: lens; and Optical window: antireflection coated window

2. EXPERIMENTAL SETUP

To observe EIT, we developed an experimental setup in which the acetylene is injected in a 1.5 m long HCPCF (Crystal Fibre, HC-1550-04), with a core diameter of 10 μm, holey region with a diameter of 75 μm, cladding pitch of about 4 μm and it has a bandgap extending over telecommunications window (C+S) of 1480–1620 nm. In Figure 1, we show the transverse cross section of the HC-PCF used in the experiments. The HC-PCF has a MFD of 9 μm, which makes this HC-PCF appropriated to be low-loss spliced with a standard SMF, due to their similar MFD and core size.

We show a schematic diagram of the experimental setup in Figure 2. The fusion splice, through its SMF section, is hermetically attached to the gas chamber, which was built with stainless steel, to avoid any unwanted reaction of acetylene with other metals. The other end of HC-PCF is just cleaved, with a high precision cleaver, and placed inside the chamber on a V-groove. The end of the HC-PCF is aligned with a collimator through an optical window, covered with antireflection coating over the entire range of the transmission window of the fiber. After passing the fiber filled with gas, the signal is then collected to be analyzed by an Optical Spectrum Analyzer.

In the following sections, we describe the splice technique, used to prepare the fiber, and the procedure applied to achieve the experimental results.

2.1. Splice Technique

One end of the HC-PCF is fusion spliced to a SMF using a Fujikura FSM-60 splicer machine. A loss of 1.5 dB was obtained. The cleaving angle obtained was smaller than 0.5°, which is important to achieve low-loss transition between HCPCF and SMF in a fusion splice. Besides that, fiber cleaning solvents were not used to avoid infiltration into the HC-PCF holes. We used a mechanical stripper and dry wiped to remove remains of the acrylate coating. The splice method is based on joining the fibers in a butt-coupling, obtaining the maximum transmission between the fibers in real time, with the help of a power-meter and a source at 1550 nm, before applying the electric discharge. The losses are determined by measuring the transmitted power before and after fusion. The splicer runs in manual alignment mode, and the electrical discharge is applied over the SMF, to avoid the collapse of the air holes [20]. We also choose a weaker fusion current and a shorter fusion time in splicing the HC-PCF and the SMF, compared with the one used in standard solid fibers [21]. We used an offset between the joint and the central axis of the arc discharge, applying the less possible amount of heat to the tip of HC-PCF, thus ensuring the preservation of the hole structure. Using the higher softening point of the SMF, we produced a resistant splice, optimizing the splicer parameters.

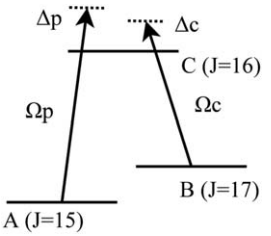

Figure 3 Energy-level scheme for the three-level lambda system, with A, B, and C representing the energy levels of the acetylene molecule. Ω_P and Δ_P are the Rabi frequency and frequency detuning for the probe-field, and Ω_C and Δ_C are the Rabi frequency and frequency detuning for the control-field

2.2. Experimental Procedure

The experimental procedure used to inject gas into the fiber was as it follows. First, we purge the fiber with acetylene and then evacuate the chamber to a pressure below 10^{-6} mbar. Afterward, we fill the chamber with 99.9% pure acetylene and detected spectroscopically the presence of gas inside the core of the fiber. All the experiments are performed between 50 and 100 mbar. The steady state is reached in less than 3 days. We use two external-cavity lasers, one tuned to 1517.31 nm, which will be our signal field, and the other tuned to 1535.39 nm, which will be our pump field, the latter one amplified by an erbium-doped fiber amplifier, and the first one passing a polarizer controller, so that we can ensure that both optical fields are copolarized. Both fields are then combined using a fiber coupler 80/20, and then launched into the fiber filled with gas, being collected by a collimator in the output to be analyzed.

The probe and control fields are tuned to the transition lines P(17) and R(15) of the acetylene [17], at 1517.31 and 1535.39 nm, respectively, between levels B and C for the latter, represented by $0\sum_g^+$ $(J = 17)$ and $v_1 + v_3\sum_u^+$ $(J = 16)$, and the former between level A, represented by $0\sum_g^+$ $(J = 15)$ and level C, as seen in Figure 3. The probe-field power is maintained below 200 μW, whereas its wavelength is scanned over the transition line R(15).

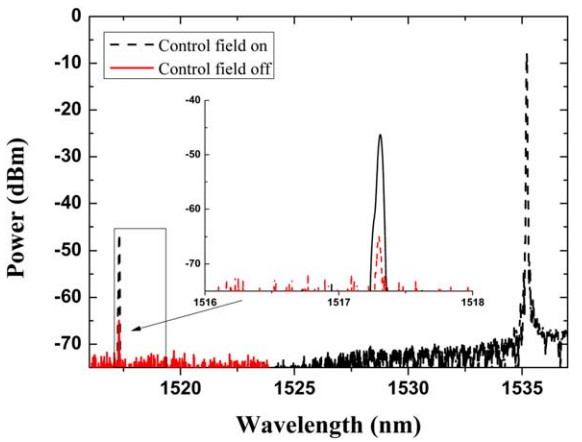

Figure 4 Transmission spectra of the probe-field signal, at 1517.31 nm, with and without control-field, at 1535.39 nm, as a function of the wavelength. [Color figure can be viewed in the online issue, which is available at wileyonlinelibrary.com]

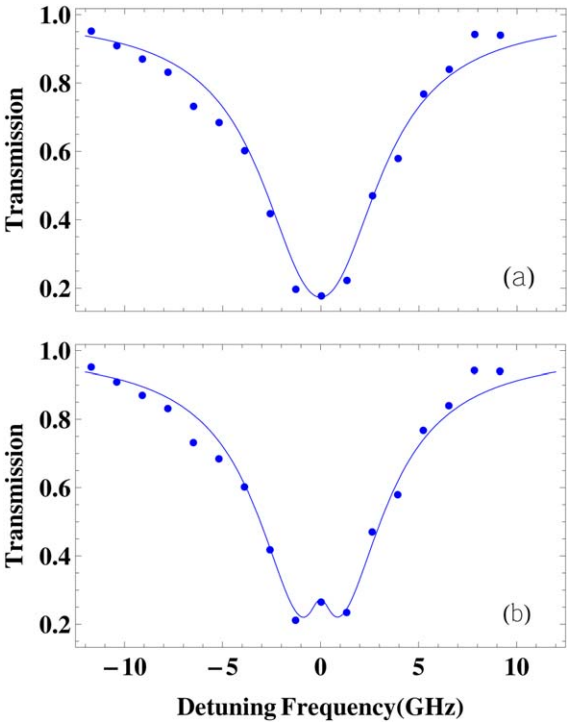

Figure 5 (a) Measured (points) and theoretical (line) doppler-broadened absorption spectra for R(15) transition in acetylene within a 1.5 m long HC-PCF. (b) Measured (points) and theoretical (lines) spectra for the same transition, but in presence of a strong control beam. [Color figure can be viewed in the online issue, which is available at wileyonlinelibrary.com]

3. RESULTS AND DISCUSSION

3.1. EIT Model

To compare our experiment with theory, we used a theoretical model, based on the following assumptions [2]: (i) the spontaneous decay from the upper state transfers the population equally between the two ground states, and is zero for the ground states, (ii) the system is closed, which means that the portion of spontaneous decay into the spectral reservoir formed by the rest of the acetylene energy states is neglected, and (iii) the effect of the probe can be ignored, as its power is very weak. Under these assumptions, the system can be described by a three-level lambda system, shown in Figure 3. Let ω_{AC} be the frequency of A–C transition and ω_{BC} be the frequency of B–C transition. The system is driven by a control-field with amplitude E_C at frequency ω_C, and by a probe-field with amplitude E_P and frequency ω_P. Solving the density-matrix equations for this system, in steady state, and considering the limit of the weak probe, we can obtain the response of the system for the probe-field. The EIT coherence for a closed three-level system is [6].

$$\rho AC = \frac{i\Omega_P}{2\left(\left(\gamma_{AC} - i\Delta_P + \frac{|\Omega_C|^2}{4(\gamma_{AB} - i(\Delta_P - \Delta_C))}\right)\right)}, \quad (1)$$

where $\Delta_P = \omega_P - \omega_{AC}$ and $\Delta_C = \omega_C - \omega_{BC}$ are the frequency detuning for probe and control-field, respectively. The Rabi frequencies, for probe and control-field, are expressed as $\Omega_P = 2_{g\ AC}E_P$ and $\Omega_C = 2_{g\ BC}E_C$, where $2\hbar g_{AC}$ and $2\hbar g_{BC}$ are the transition dipole moments for the probe and control transitions, respectively, with $\hbar$ the reduced Planck's constant. The dephasing rates are AC and AB, and it is a sum up of the contributions

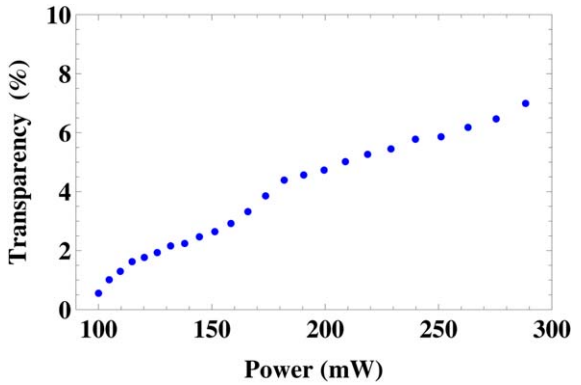

Figure 6 Experimental relative transparency as function of control-field power. [Color figure can be viewed in the online issue, which is available at wileyonlinelibrary.com]

due to collisional relaxation rates, which includes the collisions of the molecules with each other and with the fiber core wall, spontaneous decay rate and phase noise between the laser fields and laser linewidth [22]. With the approximations $\rho_{AA} \simeq 1$, $\rho_{BB} = \rho_{CC} \simeq 0$, the response of the system, for the probe-field, is determined by Eq. (1) through the susceptibility of the medium.

$$\chi = \frac{4n\hbar g_{AC}^2}{\varepsilon_0 \Omega_P} \rho_{AC}, \tag{2}$$

with n the molecular number density and ε_0 the free space permittivity, and the transmission coefficient expressed by

$$T = \frac{I_{out}}{I_{in}} = \exp\left(-k_P L \mathrm{Im}[\chi]\right), \tag{3}$$

where I_{in} is the input intensity, I_{out} the output intensity, and L is the fiber length.

3.2. Experimental Results

In Figure 4, we show the transmission spectra of the probe-field signal, with and without control-field, that is, the power transmission as function of the wavelength, at the central wavelength of the probe-field signal. In Figure 5, we show the normalized transmission profile of the probe-field, in the absence (a) and in presence of the control-field (b), as function of the frequency detuning from the central wavelength. EIT is clearly induced when the control-field is applied, leading to an increasing in the optical power of the probe-field.

We adjusted the theoretical model to the experimental data, assuming that the Rabi frequency of the control-field is constant along the fiber. Considering a control-field of 290 mW, the peak power used, we estimated a value of 9.27 MHz for Ω_c. We also estimated the molecular number density, n, and γ_{AC}, by fitting the probe-field absorption profile without the control-field, as seen in Figure 5(a). For γ_{AC} we determined a value of 1.16 GHz and 1.5×10^{19} m^{-3} for n. In Figure 5(b) we show the absorption profile in presence of the control-field. For AB, between the two lower levels, we found 506 MHz.

In Figure 6 we show the relative transparency (ratio of change in the zero-detuning of the probe transmission with control beam, to the zero-detuning of the probe transmission without the control beam), as function of the control-field power. The relative transparency increase as function of the power of the control-field, being obtained 8% of transparency, pumped with 290 mW, the maximum power we applied, corresponding to an increase of 24 nW in the probe-field. This value is low due to the pressure we used, which can produce higher values of incoherence. We observed that, due to our working pressure, the pressure broadening, in its part due to collision of the molecules with each other, dominates over the collisions of the molecules with the fiber walls. The transparency window has 1 GHz of width (FWHM). These levels of pumping powers are adequate to implement EIT in optical fiber communications, as the lasers, used on these applications, typically operate at these levels of optical power.

4. CONCLUSION

In summary, we have developed an experimental setup for EIT observation, in the telecommunications window, using acetylene molecules inside the core of a HC-PCF. This setup is suitable to work at low pumping powers due to its light launching configuration, through a low-loss splice. We obtained the typical trace of the probe-field absorption profile, without a control-field and when this is applied. It is achieved a transparency peak of about 8%, adequate to apply to lowlight applications. The theoretical model is in good agreement with our experimental measured probe-field absorption points. This model was used to determine the main parameters that characterize the coherent three-level system, such as number density and dephasing rates γ_{AB} and γ_{AC}.

REFERENCES

1. K.-J. Boller, A. Imamoglu, and S.E. Harris, Observation of electromagnetically induced transparency, Phys Rev Lett 66 (1991), 2593–2596.
2. F. Benabid, P. Light, F. Couny, and P. Russell, Electromagnetically induced transparency grid in acetylene-filled hollow-core pcf, Opt Express 13 (2005), 5694–5703.
3. S.E. Harris and Y.Yamamoto, Photon switching by quantum interference, Phys Rev Lett 81 (1998), 3611–3614.
4. H. Schmidt and R.J. Ram, All-optical wavelength converter and switch based on electromagnetically induced transparency, Appl Phys Lett 76 (2000), 22.
5. D.F. Phillips, A. Fleischhauer, A. Mair, R.L. Walsworth, and M.D. Lukin, Storage of light in atomic vapor, Phys Rev Lett 86 (2001), 783–786.
6. J. Gea-Banacloche, Y.-Q. Li, S.-Z. Jin, and M. Xiao, Electromagnetically induced transparency in ladder-type in homogeneously broadened media: Theory and experiment, Phys Rev A 51 (1995), 576–584.
7. S.E. Harris and L.V. Hau, Nonlinear optics at low light levels, Phys Rev Lett 82 (1999), 4611–4614.
8. G.S. Agarwal, T.N. Dey, and S. Menon, Knob for changing light propagation from subluminal to superluminal, Phys Rev A 64 (2001), 053809.
9. I.-H. Bae, H.S. Moon, M.-K. Kim, L. Lee, and J.B. Kim, Transformation of electromagnetically induced transparency into enhanced absorption with a standing-wave coupling field in an rb vapor cell, Opt Express 18 (2010), 1389–1397.
10. M.V. Pack, R.M. Camacho, and J.C. Howell, Transients of the electromagnetically-induced-transparency-enhanced refractive kerr nonlinearity, Phys Rev A 76 (2007), 033835.
11. S. Ghosh, J.E. Sharping, D.G. Ouzounov, and A.L. Gaeta, Resonant optical interactions with molecules confined in photonic band-gap fibers, Phys Rev Lett 94 (2005), 093902.
12. F. Benabid, J.C. Knight, G. Antonopoulos, and P.S.J. Russell, Stimulated raman scattering in hydrogen-filled hollow-core photonic crystal fiber, Science 298 (2002), 399–402.

13. S.O. Konorov, A.B. Fedotov, and A.M. Zheltikov, Enhanced four-wave mixing in a hollow-core photonic-crystal fiber, Opt Lett 28 (2003), 1448–1450.
14. M. Nisoli, S.D. Silvestri, O. Svelto, R. Szipöcs, K. Ferencz, C. Spielmann, S. Sartania, and F. Krausz, Compression of high-energy laser pulses below 5 fs, Opt Lett 22 (1997), 522–524.
15. M. Bajcsy, S. Hofferberth, V. Balic, T. Peyronel, M. Hafezi, A.S. Zibrov, V. Vuletic, and M.D. Lukin, Efficient all-optical switching using slow light within a hollow fiber, Phys Rev Lett 102 (2009), 203902.
16. W.C. Swann and S.L. Gilbert, Pressure-induced shift and broadening of 1510–1540-nm acetylene wavelength calibration lines, J Opt Soc Am B 17 (2000), 1263–1270.
17. K. Keppler, G. Mellau, S. Klee, B. Winnewisser, M. Winnewisser, J. Pliva, and K. Rao, Precision measurements of acetylene spectra at 1.4 μm 1.7 μm recorded with 352.5-m pathlength, J Mol Spectrosc 175 (1996), 411–420.
18. P.S. Light, Photonic microcells for quantum applications, PhD Thesis, Department of Physics, University of Bath, May 2008.
19. N. Wheeler, P. Light, F. Couny, and F. Benabid, Slow and superluminal light pulses via EIT in a 20-m acetylene-filled photonic microcell, J Lightwave Technol 28 (2010), 870–875.
20. L. Xiao, M. Demokan, W. Jin, Y. Wang, and C. Zhao, Fusion splicing photonic crystal fibers and conventional single-mode fibers: Microhole collapse effect, J Lightwave Technol 25 (2007), 3563–3574.
21. B.D. Tiburcio, G.M. Fernandes, and A.N. Pinto, Extremely small-core photonic crystal fiber fusion splicing with a single-mode fiber, In: Proc SPIE, vol. 8785. 8th Iberoamerican Optics Meeting and 11th Latin American Meeting on Optics, Lasers, and Applications, 2013, pp. 8785FF–8785FF–6.
22. E. Arimondo, Relaxation processes in coherent-population trapping, Phys Rev A 54 (1996), 2216–2223.

AN INVESTIGATION ON TRANSIENT EFFECTS IN EDFA WITH VARIABLE DUTY CYCLE AND WAVELENGTH MULTIPLEXED SIGNALS

Meena Dasan,[1,2] Sarath Thodiyil,[3] Fredy Francis,[3] Dipin Elambilayi,[3] and Srinivas Talabattula[1]
[1] Electrical Communication Engineering, Indian Institute of Science, India; Corresponding author: dmeenasatish@gmail.com
[2] Electronics and Radar Development Establishment, India
[3] Department of Electronics Engineering, Model Engineering College, India

Received 4 July 2014

ABSTRACT: *The advent of erbium doped fiber amplifiers (EDFA) has revolutionized optical communication in the past few decades. Traditionally, it was being used with relatively high bitrates system for amplification in the optical domain. The slow gain response of EDFA is inherently resistant to transient effects from bit rate and duty cycle variations in high bit rate optical systems. We investigate the transient effects of EDFA on low bitrate systems with variable duty cycle and pump power configurations. Also, the effect of transients in WDM multirate systems has been investigated. The work is supported with both simulation and experimental results.* © 2015 Wiley Periodicals, Inc.
Microwave Opt Technol Lett 57:352–356, 2015; View this article online at wileyonlinelibrary.com. DOI 10.1002/mop.28845

Key words: *erbium doped fiber amplifiers; variable duty cycle; transients; low bit rate*

1. INTRODUCTION

Erbium doped fiber amplifier (EDFA) systems widely used in optical amplification of communication signals have been actively investigated for various effects, since its invention in the early 1990s. As these were primarily limited to high speed applications, during the early days most of the research have been focused in tuning EDFA to work at high bit rates for different wavelengths simultaneously. But with optical systems finding its way to diverse fields, various scenarios yet to be explored with EDFA have emerged. One such scenario is the transmission of low bit rate control signals over fiber link for radar applications. This typically involve the transmission of variable duty cycle signal at relatively low pulse rate. As EDFA is slow with regard to gain recovery, it do affect the way low frequency signals are amplified.

EDFA is generally analyzed based on a three level energy model, the pump laser excites the erbium ions into the upper level, where it gets immediately decayed into a metastable state with a few microseconds. The lifetime at the metastable state is relatively longer, around 10 ms, making the erbium ions to accumulate over time providing a buffer action, which makes EDFA practically resistant to gain fluctuations during amplification at high bitrate signals. But with signals having pulse width comparable to the erbium ion life time, EDFA gain shows transient effects, which can adversely affect signal amplification at the lower bitrates.

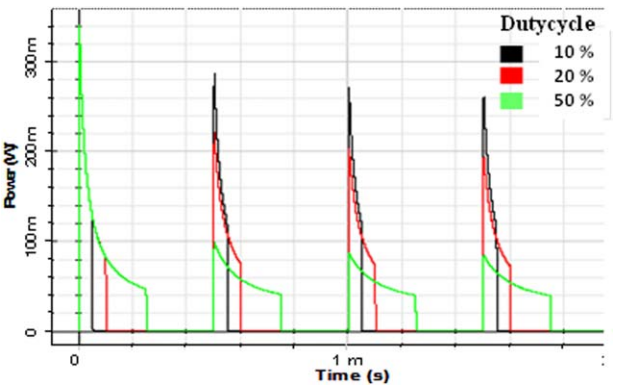

Figure 1 EDFA transients with 10, 20, and 50% duty cycle (2 KHz pulsed signals, pump power at 60 mW). [Color figure can be viewed in the online issue, which is available at wileyonlinelibrary.com]

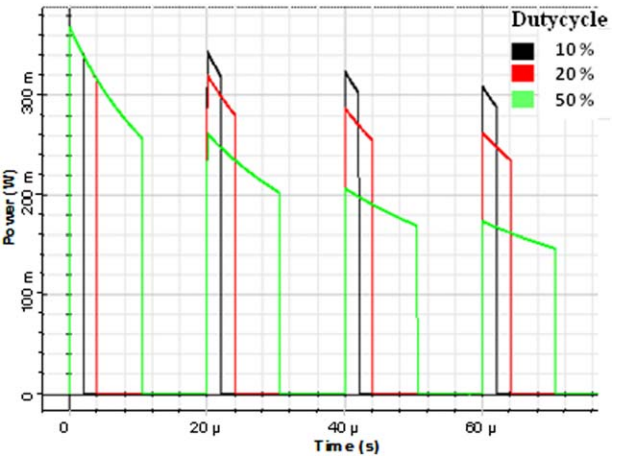

Figure 2 EDFA transients for higher bit rate signal (50 KHz pulsed signals, 60 mW pump power). [Color figure can be viewed in the online issue, which is available at wileyonlinelibrary.com]